

# High spatial resolution measurements of NO<sub>2</sub> applying Topographic Target Light scattering-Differential Optical Absorption Spectroscopy (ToTaL-DOAS)

E. Frins<sup>1</sup>, U. Platt<sup>2</sup>, and T. Wagner<sup>3</sup>

<sup>1</sup>Instituto de Física, Facultad de Ingeniería, J. Herrera y Reissig 565, 11300 Montevideo, Uruguay

<sup>2</sup>Institut für Umweltp Physik, University of Heidelberg, Im Neuenheimer Feld 229, 69120 Heidelberg, Germany

<sup>3</sup>Max-Planck-Institut für Chemie, Becherweg 27, 55128 Mainz, Germany

Received: 15 April 2008 – Accepted: 21 April 2008 – Published: 2 June 2008

Correspondence to: E. Frins (efrins@fing.edu.uy)

Published by Copernicus Publications on behalf of the European Geosciences Union.

High spatial  
resolution  
measurements with  
ToTaL-DOAS

E. Frins et al.

Title Page

Abstract

Introduction

Conclusions

References

Tables

Figures

⏪

⏩

◀

▶

Back

Close

Full Screen / Esc

Printer-friendly Version

Interactive Discussion

## Abstract

Tomographic Target Light scattering – Differential Optical Absorption Spectroscopy (ToTaL-DOAS), also called Target-DOAS, is a novel experimental procedure to retrieve trace gas concentrations present in the low atmosphere. Scattered sunlight (partially or totally) reflected from natural or artificial targets of similar albedo located at different distances is analyzed to retrieve the concentration of different trace gases like NO<sub>2</sub>, SO<sub>2</sub> and others. We report high spatial resolution measurements of NO<sub>2</sub> mixing ratios in the city of Montevideo (Uruguay) observing three buildings as targets with a Mini-DOAS instrument. Our instrument was 146 m apart from the first building, 196 m from the second and 286 m from the third one. All three buildings are located along a main Avenue. We obtain temporal variation of NO<sub>2</sub> mixing ratios between 30 ppb and 65 ppb ( $\pm 2$  ppb). Our measurements demonstrate that ToTaL-DOAS measurements can be made over very short distances. In polluted air masses, the retrieved absorption signal was found to be strong enough to allow measurements over distances in the range of several ten meters, and achieve a spatial resolution of 50 m approximately.

## 1 Introduction

Monitoring dispersion of trace gases in the troposphere near the earth surface is a challenge, particularly when mobile emission sources are involved and the area of interest has complicated structures. This is usually the case in the surrounding of a busy road in a city. High temporal and spatial resolution is desirable to describe trace gas dispersion in the site properly. The first requirement is achieved by several passive and active optical detection methods. The second condition, i.e. the spatial resolution, is also fulfilled by some very well established optical techniques like LIDAR (e.g. Collis, 1996; Klett, 1981; Fernald, 1984) and Tomographic-DOAS (see e.g. Veitel et al., 2002; Laepple et al., 2004; Pundt et al., 2005; Hartl et al., 2006; Hashmonay et al., 1999). Unfortunately their application is associated with high expenses and staff requirements.

ACPD

8, 10257–10273, 2008

### High spatial resolution measurements with ToTaL-DOAS

E. Frins et al.

Title Page

Abstract

Introduction

Conclusions

References

Tables

Figures

⏪

⏩

◀

▶

Back

Close

Full Screen / Esc

Printer-friendly Version

Interactive Discussion

---

**High spatial  
resolution  
measurements with  
ToTaL-DOAS**

---

E. Frins et al.

[Title Page](#)[Abstract](#)[Introduction](#)[Conclusions](#)[References](#)[Tables](#)[Figures](#)[⏪](#)[⏩](#)[◀](#)[▶](#)[Back](#)[Close](#)[Full Screen / Esc](#)[Printer-friendly Version](#)[Interactive Discussion](#)

Topographic Target Light scattering-DOAS (ToTaL-DOAS or Target-DOAS) (Frins et al., 2006a, b, and Louban et al., 2007) is a new experimental procedure to retrieve trace gas concentrations in the atmosphere near the earth surface. Basically, the method consists of pointing a DOAS instrument at different targets, which are illuminated by direct and/or scattered sun light. Applying a DOAS analysis to the obtained spectra one retrieves the slant column densities (the integrated trace gas concentration) along several segments of known length, which, in turn, allows us to derive the average trace gas concentrations. The spectral analysis varies depending on the number and sort of selected targets (bright, mixed or dark targets). A detailed description of the method is given in Frins et al. (2006a).

In early works we reported the application of this method to very large sites (Frins et al., 2006a) and to remote measurements (Louban et al., 2007), i.e. sites located far away from our instrument. The purpose of the present work is to explore the spatial resolution of ToTaL-DOAS using targets at short distances.

## 2 ToTaL-DOAS measurements

### 2.1 Site description and instrument

We selected as area of interest a main street of Montevideo city (Italia Avenue), which is predominantly affected by mobile sources, since it is used by most of the private and public transport means to drive in and out of the city. On 6 November 2007 measurements were made with a Mini MAX-DOAS instrument (Bobrowski, 2005 and Bobrowski et al., 2007) Basically, the instrument consists of a small commercial temperature controlled fibre-optic spectrometer with a spectral resolution of 0.55 nm and a spectral range from 330–460 nm. To reduce the dark current of the detector the entire spectrometer was cooled to a stabilised temperature of +6°C. The light is coupled into the spectrometer through a quartz lens ( $f=40$  mm, diameter=20 mm) and a quartz fibre bundle. The field of view is approximately 0.4°. The instrument is mounted on a tripod

and can be moved to point at different targets. It can also be oriented to elevation angles between  $0^\circ$  and  $90^\circ$  approximately. To make sure that our instrument was pointing to a specific Target, a reflex sight was installed.

We located our instrument in a Park at one side of Ave. Italia, approximately 22 m ( $\pm 2$  m) away from the border of the lane (Fig. 1a). Three (almost) white walls of three different buildings at the other side of the street were selected as bright targets, i.e. the radiance reflected by these targets is assumed to be much higher than that due to sunlight scattering coming from the region between targets and instrument. These buildings were located at 146 m ( $\pm 2$  m), 196 m ( $\pm 2$  m) and 280 m ( $\pm 2$  m) apart from our instrument (Fig. 1b). We will call these buildings as target 1, target 2 and target 3, respectively.

The measurements were performed by alternating the view between the three far targets, i.e. three selected walls of the buildings, the near target (three small pieces of different concrete, see below), and a zenith measurement. During the measurement period the ambient temperature was about  $28^\circ\text{C}$ . In addition, dark current and offset measurements under the same conditions were taken. The data acquisition was performed with the software package DOASIS (see [www.iup.uni-heidelberg.de/bugtracker/projects/doasis/](http://www.iup.uni-heidelberg.de/bugtracker/projects/doasis/)).

## 2.2 Spectral analysis

In order to retrieve the integrated trace gas concentration along the paths between our instrument and the targets, we decided to use a near target at a distance  $d \approx 0$  m from the instrument to record a reference spectrum instead using a zenith sky spectrum. For this purpose, we tested three casually available pieces of concrete. Like the far targets 1, 2 and 3 (white painted walls), also the used pieces of concrete were for long time exposed to the same ambient conditions, so it was expected that their spectral reflectivity might also be similar. This assumption was tested by inspecting the spectral residuals from the various combinations of measurements (spectra from the buildings) and reference spectra (spectra from the pieces of concrete). It was found that for sev-

Title Page

Abstract

Introduction

Conclusions

References

Tables

Figures

◀

▶

◀

▶

Back

Close

Full Screen / Esc

Printer-friendly Version

Interactive Discussion



5 eral combinations strongly increasing residual structures (up to more than 2%) towards shorter wavelengths appeared (Fig. 2). Similar results were found if the various target spectra were analysed against the zenith sky spectrum. No clear dependence of the magnitude of the residual structures and the properties of the targets was found from our limited set of combinations. The systematic analysis of the spectral reflectivity of various materials and paints should be the subject of future studies.

The spectral region for the evaluation of NO<sub>2</sub> was selected considering simultaneously two conditions: 1) the absorption cross section is high enough and 2) the residual is small, i.e. the spectral structure caused by the different spectral reflectances does not interfere with our measurements. For example, Fig. 2 shows a NO<sub>2</sub>-evaluation using the third building as target and a piece of concrete as reference; clearly, the residual decreases towards longer wavelengths (see details below). Taking in account these considerations, the spectral range for the evaluation of NO<sub>2</sub> was chosen between 429 nm and 460 nm.

15 The NO<sub>2</sub> slant column densities (SCD), i.e. the integrated concentration along the light path between targets (target 1, 2 and 3) and instrument (Mini MAX-DOAS), were derived from the spectral analysis using the software WINDOAS package (Fayt et al., 2001). The absorption cross sections of O<sub>4</sub> (Greenblatt et al., 1990) and NO<sub>2</sub> (Vandale et al., 1997) at 294 K, O<sub>3</sub> (Burrows et al., 1999) at 273 K and water vapor at 300 K (Rothman et al., 2005) were fitted to the logarithm of the ratios between the measured spectra of the targets and the reference spectrum. Additionally a synthetic Ring spectrum was included in the evaluation. As shown in Fig. 2, the NO<sub>2</sub> absorption could be clearly identified in the measured spectra indicating that in polluted air masses rather short absorption paths are sufficient to achieve a good signal to noise ratio. From our observations it appears to be possible to further reduce the distance between instrument and target (i.e. the absorption pathlength). Assuming a detection limit from the DOAS analysis for the NO<sub>2</sub> SCD of about 10<sup>15</sup> molec/cm<sup>2</sup>, the corresponding detection limit of the NO<sub>2</sub> mixing ratio for an absorption path of only 50 m would be about 8 ppb. It should be noted here that in the future, the DOAS analysis might be significantly im-

---

## High spatial resolution measurements with ToTaL-DOAS

E. Frins et al.

---

Title Page

Abstract

Introduction

Conclusions

References

Tables

Figures

⏪

⏩

◀

▶

Back

Close

Full Screen / Esc

Printer-friendly Version

Interactive Discussion

proved (e.g. by using selected materials for the measurement of a reference spectrum) and accordingly the detection limit can be further decreased.

### 2.3 Interpretation of the analyzed slant column densities

In first approximation, the retrieved slant column density represents the integrated trace gas concentration between the target and the instrument. This interpretation is based on the assumption that the trace gas absorptions between the top of the atmosphere and the targets (either far targets, e.g. buildings or near Target, e.g. a piece of concrete) are similar and thus cancel out when rationing spectra from any of the far targets by one from the near target in the DOAS analysis. While this assumption should be quite well justified for absorptions in the upper troposphere and stratosphere, it might not be fulfilled for the trace gas absorptions close to the surface, where strong 3-dimensional gradients can occur. The potential errors introduced by such gradients are discussed and estimated in the following.

Considering the location of our instrument and the position of the targets relative to the extended emission source, there are different scenarios to be considered and could affect our interpretation: a) the emission cloud is separated from the target walls and also separated from our instrument, as depicted in Fig. 3a; b) the emission cloud encompasses the far Target, so a fraction of the sunlight scattered from the targets contains additional absorption from the light path before the sun light has reached the target (Fig. 3b); c) the instrument (i.e. the near Target) is reached by the emission cloud (Fig. 3c), and d) the target and our instrument are partially immersed in the emission cloud (Fig. 3d). In cases a) and d) the retrieved slant column density represents the true slant column density between the Target and the instrument. In case b) the measured SCD overestimates the true SCD and in case c) it underestimates the true SCD. The associated error can be quantified by estimating the maximum difference in the vertical extension of the plume on both ends of the light path. Assuming a maximum difference of 20 m yields an error of the retrieved SCD between 13% and 8% for target 1 and target 3, respectively. It is evident that the relative magnitude of this error source depends on

**High spatial resolution measurements with ToTaL-DOAS**

E. Frins et al.

Title Page

Abstract

Introduction

Conclusions

References

Tables

Figures



Back

Close

Full Screen / Esc

Printer-friendly Version

Interactive Discussion



the ratio of the uncertainty in the vertical extent of the plume and the distance to the far Target.

In particular it decreases with increasing distance between the instrument and the far Target.

From the retrieved SCD the average concentration is simply derived by dividing the SCD by the distance between instrument and Target. Dividing the obtained concentration by the concentration of air yields the averaging mixing ratio. In the following we report average NO<sub>2</sub> mixing ratios derived in this way.

Figure 4 shows the temporal evolution of the NO<sub>2</sub> mixing ratios obtained by the three different paths. As mentioned before, the measurement took place alternating between the different targets. From the (four) first measurements (instrument pointing to target 1) one observes a small increase of the NO<sub>2</sub> mixing ratio from 30 ppb ( $\pm 2$  ppb) to 41 ppb ( $\pm 1$  ppb). As the instrument is directed to targets 2 and 3, the evaluation shows a stronger increase of the NO<sub>2</sub> mixing ratio (52 ppb and 65 ppb, respectively). This NO<sub>2</sub> increase is probably not due to the particular location of the targets (e.g. it is not due to a spatially inhomogeneous concentration distribution), which was verified by pointing the instrument again to target 1, which yielded similar high values. Some minutes later again a decrease of the NO<sub>2</sub> mixing ratio was observed (see last measurement in Fig. 4). Temporal variations of the NO<sub>2</sub> mixing ratios may be interpreted as a consequence of the passage of heavy vehicles like buses or trucks.

The resulting slant column densities, concentration and mixing ratios of NO<sub>2</sub> measured between 17:34 and 17:38 LT for the different paths is summarized in Table 1.

### 3 Discussion and conclusions

In this paper we report measurements of NO<sub>2</sub> mixing ratios in the city of Montevideo (Uruguay) applying the ToTaL-DOAS method. We used three buildings located along a main Avenue as targets. Our Mini-DOAS instrument was only 146 m apart from the first building, 196 m from the second and 286 m from the third one.

**High spatial  
resolution  
measurements with  
ToTaL-DOAS**

E. Frins et al.

Title Page

Abstract

Introduction

Conclusions

References

Tables

Figures

⏪

⏩

◀

▶

Back

Close

Full Screen / Esc

Printer-friendly Version

Interactive Discussion

The first step for the evaluation of NO<sub>2</sub> mixing ratios was the determination of slant column densities along the segments between instrument and targets. Then, assuming that the NO<sub>2</sub> concentration is spatially constant in the region of interest (apart from the instrument and targets) and knowing the distance between instrument and (far) targets, it is possible to retrieve the NO<sub>2</sub> mixing ratios.

It was found that the calculated mixing ratios obtained from the shorter path (Target 1) shows a standard deviation ~3.2–5%, which is larger than the standard deviations associated to measurements using longer path lengths (1.5% for target 2 and 0.8% for target 3). This is physically reasonable because the magnitudes actually measured are the optical densities along the light paths, and thus, the signal-to-noise ratio will be smaller for the longer path lengths.

Usually a zenith spectrum is used as reference spectrum. Instead of this, we used as reference the spectrum of a near target (in our case a piece of concrete, see above) placed at a distance  $d \approx 0$  m from the instrument. We found that some of the available pieces of concrete, exposed for long time to the same ambient conditions like the buildings (targets), have a similar spectral reflectance to those of the targets, allowing a good convergence of the spectral DOAS retrieval in the spectral range 429–460 nm. However, it should be noted that the spectral reflectances of the different targets (buildings and various pieces of concrete) showed significant differences in the wavelength ranges <430 nm. These effects should be studied in more detail in the future; probably well suited reference materials can be identified for various types of buildings and paintings to allow also a meaningful DOAS retrieval at shorter wavelengths. Alternatively, artificial, diffuse reflecting targets may be attached to buildings. From the spectral residuals of our DOAS analysis we conclude that in polluted air masses, ToTaL-DOAS measurements are possible over very short distances in the range of several ten meters.

Furthermore, using as reference the spectrum obtained from one of the targets, it is possible to apply the ToTaL-DOAS method to evaluate trace gas concentrations in the region between several far targets. Using a well suited set of targets, it will be easily

---

## High spatial resolution measurements with ToTaL-DOAS

E. Frins et al.

---

Title Page

Abstract

Introduction

Conclusions

References

Tables

Figures

⏪

⏩

◀

▶

Back

Close

Full Screen / Esc

Printer-friendly Version

Interactive Discussion



possible to apply tomographic techniques and to retrieve trace gas distributions in two or three dimensions (Hartl et al., 2006; Hashmonay et al., 1999).

Also, since the radiance received by the Mini-DOAS instrument was sufficiently high, the acquisition times were short, ranging only between 1 and 3 min depending on the target. Thus, in addition to the spatial resolution of the method, a considerable temporal resolution can be achieved. We measured temporal variation of NO<sub>2</sub> mixing ratios between 30 ppb and 65 ppb ( $\pm 2$  ppb) in a time interval of 45 min.

*Acknowledgements.* E. Frins acknowledges PEDECIBA-Física (Project URU/06/004) for providing partial financial support.

## References

Bobrowski, N.: Volcanic Gas Studies by Multi Axis Differential Optical Absorption Spectroscopy, Doctoral Thesis, University of Heidelberg, Germany, 2005.

Bobrowski, N. and Platt, U.: SO<sub>2</sub>/BrO ratios studied in five volcanic plumes, J. Volcanol. Geotherm. Res., 166, 3–4, 147–160, doi:10.1016/j.jvolgeores.2007.07.003, 2007.

Burrows, J. P., Dehn, A., Deters, B., Himmelmann, S., Richter, A., Voigt, S., and Orphal, J.: Atmospheric Remote-Sensing Reference Data from GOME: 2. Temperature-Dependent Absorption Cross Sections of O<sub>3</sub> in the 231–794 nm Range, J. Quant. Spectrosc. Rad. Trans., 61, 509–517, 1999.

Collis, R. T. H.: Lidar: a new atmospheric probe, Q. J. Roy. Meteorol. Soc., 92, 220–230, 1966.

Fernald, F. G.: Analysis of atmospheric LIDAR observations: Some comments, Appl. Optics, 23, 652–653, 1984.

Frins, E., Bobrowski, N., Platt, U., and Wagner, T.: Tomographic multiaxis-differential optical absorption spectroscopy observations of Sun-illuminated targets: a technique providing well-defined absorption paths in the boundary layer, Appl. Optics, 45, 6227–6240, 2006a.

Frins, E., Bobrowski, N., Platt, U., and Wagner, T.: Thomographic MAX-DOAS Observations of Sun Illuminated Targets: A New Technique Providing Well Defined Absorption Paths in the Boundary Layer or simply: Topographic Target Light scattering – DOAS ToTal – DOAS, Third International DOAS Workshop, Bremen, Germany, 2006b.

**High spatial  
resolution  
measurements with  
ToTal-DOAS**

E. Frins et al.

Title Page

Abstract

Introduction

Conclusions

References

Tables

Figures

⏪

⏩

◀

▶

Back

Close

Full Screen / Esc

Printer-friendly Version

Interactive Discussion

---

**High spatial  
resolution  
measurements with  
ToTaL-DOAS**E. Frins et al.

---

Title Page

Abstract

Introduction

Conclusions

References

Tables

Figures

⏪

⏩

◀

▶

Back

Close

Full Screen / Esc

Printer-friendly Version

Interactive Discussion

Greenblatt G. D., Orlando, J. J., Burkholder, J. B., and Ravishankara, A. R.: Absorption measurements of oxygen between 330 and 1140 nm, *J. Geophys. Res.*, 95, 18577–18582, 1990.

Hartl A., Song B. C., and Pundt, I.: 2-D reconstruction of atmospheric concentration peaks from horizontal long path DOAS tomographic measurements: parametrisation and geometry within a discrete approach, *Atmos. Chem. Phys.*, 6, 847–861, 2006,  
<http://www.atmos-chem-phys.net/6/847/2006/>.

Hashmonay, R. A., Yost, M. G., and Wu, C. F.: Computed Tomography of Air Pollutants Using Radial Scanning Path-Integrated Optical Remote Sensing. *Atmos. Environ.*, 33, 267–274, 1999.

Klett, J. D.: Stable analytical inversion solution for processing LIDAR returns, *Appl. Optics*, 20, 211–220, 1981.

Laepple, T., Knab, V., Mettendorf, K. U., and Pundt, I.: Longpath DOAS tomography on a motorway exhaust plume: Numerical studies and application to data from the BAB II campaign, *Atmos. Chem. Phys.*, 4, 1323–1342, 2004,  
<http://www.atmos-chem-phys.net/4/1323/2004/>.

Louban, I., Píriz, G., Platt, U., and Frins, E.: Differential Optical Absorption Spectroscopy (DOAS) using targets: SO<sub>2</sub> and NO<sub>2</sub> measurements in Montevideo city, AIP Conference Proceeding, 992, 21–26, RIAO/OPTILAS, 2007.

Pundt, I., Mettendorf, K.U., Laepple, T., Knab, V., Xie, P., Lösch, J., v. Friedeburg, C., Platt, U., and Wagner, T.: Measurements of trace gas distributions using long-path DOAS-tomography during the motorway campaign BAB II: Experimental setup and results for NO<sub>2</sub>, *Atmos. Environ.*, 39, 967–975, 2005.

Rothman, L.S., Jacquemart, D., Brown, L. R., Carleer, M., Gamache, R. R., et al.: The HITRAN 2004 Molecular Spectroscopic Database, *J. Quant. Spectrosc. Rad. Transf.*, 96, 139–204, 2005.

Vandaele, A. C., Hermans, C., Simon, P. C., Carleer, M., Colin, R., Fally, S., Mérienne, M.-F., Jenouvrier, A., and Coquart, B.: Measurements of the NO<sub>2</sub> absorption cross section from 42 000 cm<sup>-1</sup> to 10 000 cm<sup>-1</sup> (238–1000 nm) at 220 K and 294 K, *J. Quant. Spectrosc. Radiat. Transf.*, 59, 171–184, 1997.

Veitel, H., Kromer, B., Mößner, M., and Platt, U.: New techniques for measurements of atmospheric vertical trace gas profiles using DOAS, *Environ. Sci. Pollut. Res.*, 4, 17–26, 2002.

## High spatial resolution measurements with ToTaL-DOAS

E. Frins et al.

**Table 1.** Measured NO<sub>2</sub> mixing ratios.

Target (referred to target at $d=0$ m)	Local time	Slant Column Density [molec/cm <sup>2</sup> ]	Concentration [molec./cm <sup>3</sup> ]	Mixing Ratio [ppb]
Target 2 (196 m)	17:34	$2.47 \times 10^{16} \pm 3.6 \times 10^{14}$	$1.26 \times 10^{12} \pm 1.8 \times 10^{10}$	52±1
Target 3 (286 m)	17:36	$4.52 \times 10^{16} \pm 3.6 \times 10^{14}$	$1.58 \times 10^{12} \pm 1.3 \times 10^{10}$	65±1
Target 1 (146 m)	17:38	$2.32 \times 10^{16} \pm 8.4 \times 10^{14}$	$1.59 \times 10^{12} \pm 5.7 \times 10^{10}$	65±2

Title Page

Abstract

Introduction

Conclusions

References

Tables

Figures

⏪

⏩

◀

▶

Back

Close

Full Screen / Esc

Printer-friendly Version

Interactive Discussion

---

**High spatial  
resolution  
measurements with  
ToTaL-DOAS**E. Frins et al.

---

[Title Page](#)[Abstract](#)[Introduction](#)[Conclusions](#)[References](#)[Tables](#)[Figures](#)[⏪](#)[⏩](#)[◀](#)[▶](#)[Back](#)[Close](#)[Full Screen / Esc](#)[Printer-friendly Version](#)[Interactive Discussion](#)

**Fig. 1. (a)** View of the site from above, taken from [www.googleearth.com](http://www.googleearth.com). The arrows indicate the position of targets 1, 2 and 3, respectively. The Mini-DOAS instrument is located at the origin of the arrows.

---

**High spatial  
resolution  
measurements with  
ToTaL-DOAS**

E. Frins et al.



**Fig. 1. (b)** View of the targets from the instrument location.

[Title Page](#)[Abstract](#)[Introduction](#)[Conclusions](#)[References](#)[Tables](#)[Figures](#)[◀](#)[▶](#)[◀](#)[▶](#)[Back](#)[Close](#)[Full Screen / Esc](#)[Printer-friendly Version](#)[Interactive Discussion](#)

**High spatial  
resolution  
measurements with  
ToTaL-DOAS**

E. Frins et al.

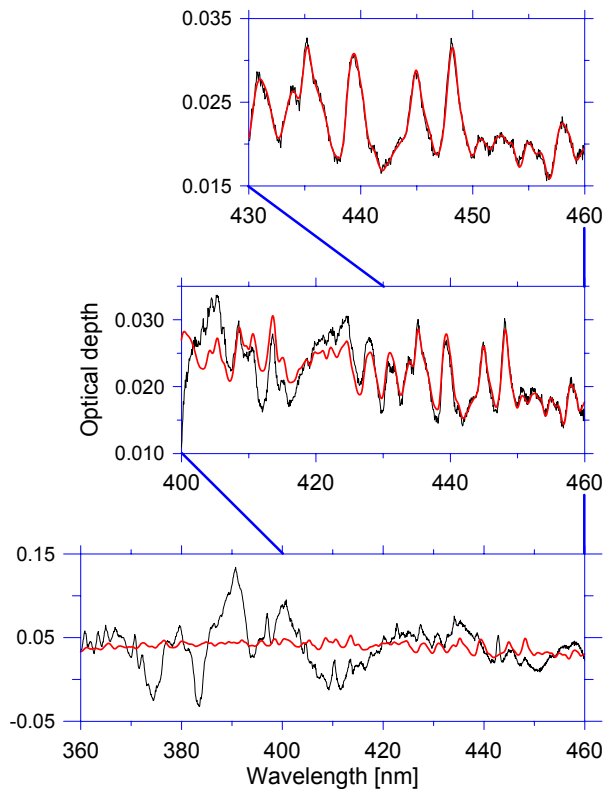


**Fig. 2.** Test analysis to find out the optimal spectral region for  $\text{NO}_2$  evaluation against a piece of concrete.

[Title Page](#)[Abstract](#)[Introduction](#)[Conclusions](#)[References](#)[Tables](#)[Figures](#)[◀](#)[▶](#)[◀](#)[▶](#)[Back](#)[Close](#)[Full Screen / Esc](#)[Printer-friendly Version](#)[Interactive Discussion](#)

High spatial  
resolution  
measurements with  
ToTaL-DOAS

E. Frins et al.

Title Page

Abstract

Introduction

Conclusions

References

Tables

Figures

◀

▶

◀

▶

Back

Close

Full Screen / Esc

Printer-friendly Version

Interactive Discussion

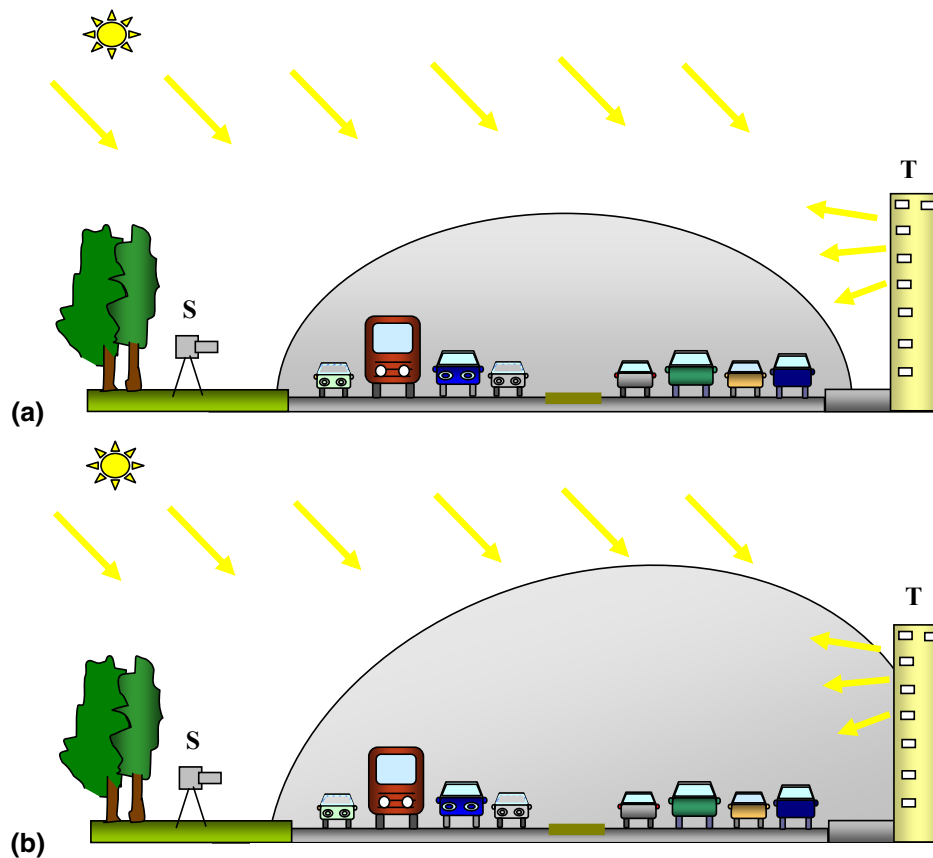


**Fig. 3.** Different scenarios to be considered: **(a)** Emission cloud separated from the target (T) walls and from the instrument (S). **(b)** Target (T) immersed in the emission cloud.

**High spatial  
resolution  
measurements with  
ToTal-DOAS**

E. Frins et al.

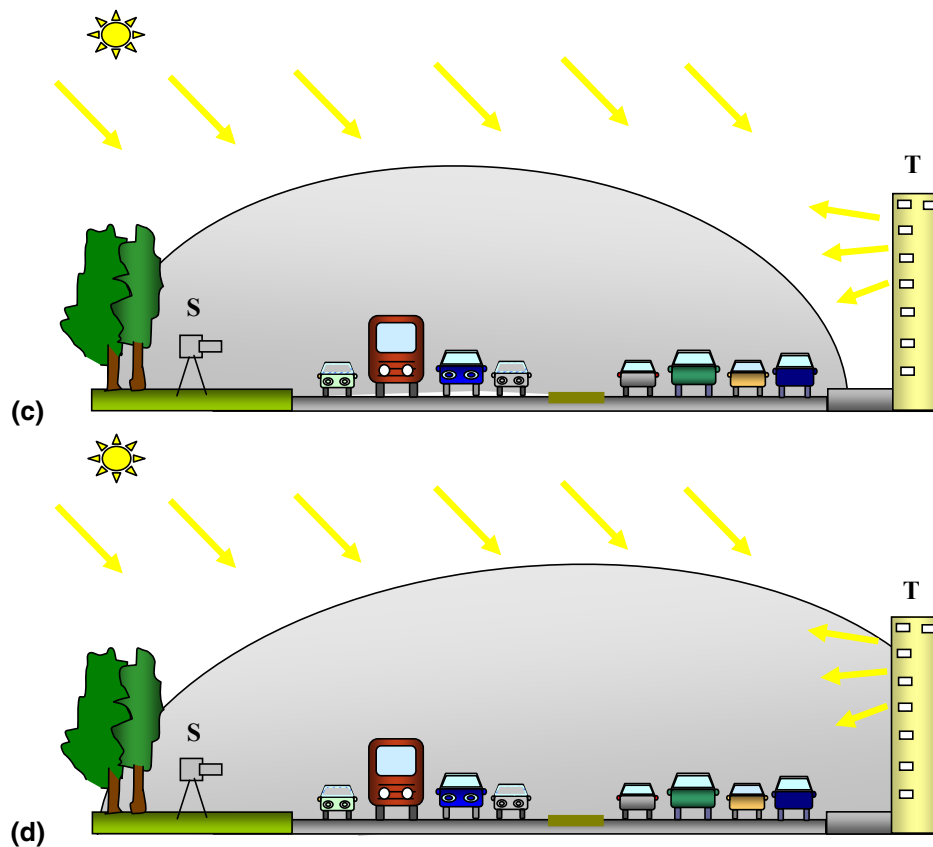


**Fig. 3.** (c) Instrument (I) immersed in the emission cloud. (d) Target (T) and instrument (S) are immersed in the emission cloud.

[Title Page](#)[Abstract](#)[Introduction](#)[Conclusions](#)[References](#)[Tables](#)[Figures](#)[◀](#)[▶](#)[◀](#)[▶](#)[Back](#)[Close](#)[Full Screen / Esc](#)[Printer-friendly Version](#)[Interactive Discussion](#)



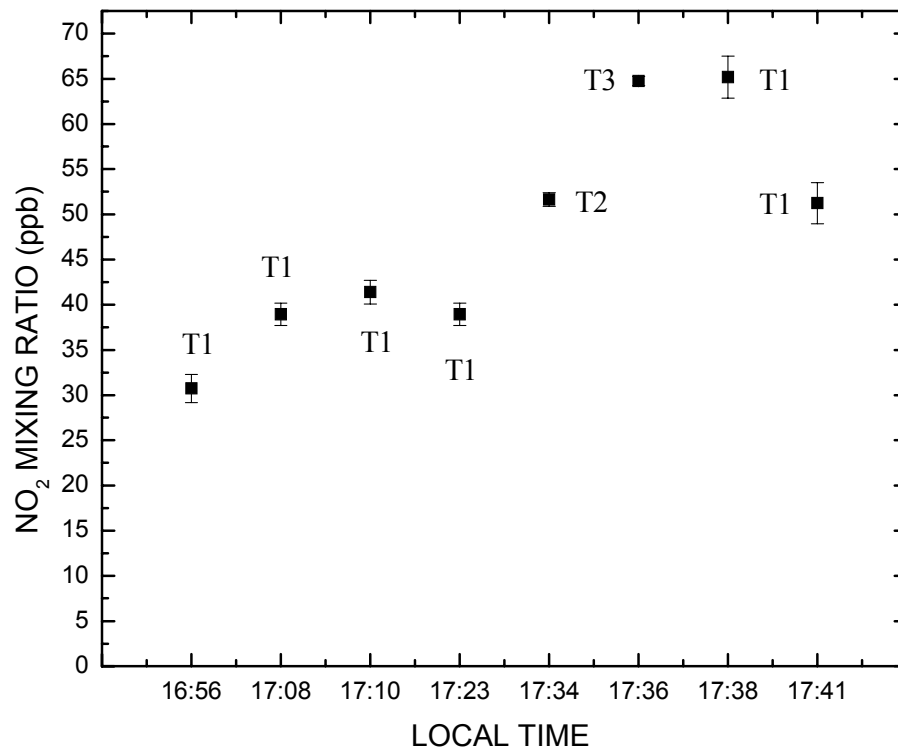


**Fig. 4.** Time evolution of the NO<sub>2</sub> mixing ratio. T1–T3 denote measurements with the instrument pointing to target 1, 2, and 3, respectively.

[Title Page](#)[Abstract](#)[Introduction](#)[Conclusions](#)[References](#)[Tables](#)[Figures](#)[⏪](#)[⏩](#)[◀](#)[▶](#)[Back](#)[Close](#)[Full Screen / Esc](#)[Printer-friendly Version](#)[Interactive Discussion](#)